Title
Ohmic Contact to p-Type GaN Enabled by Post-Growth Diffusion of Magnesium

Journal
IEEE Electron Device Letters, 43(1)

ISSN
0741-3106

Authors
Wang, Jia
Lu, Shun
Cai, Wentao
et al.

Publication Date
2022

DOI
10.1109/led.2021.3131057

Peer reviewed

Ohmic Contact to *p*-Type GaN Enabled by Post-Growth Diffusion of Magnesium

Jia Wang, Shun Lu, Wentao Cai, Takeru Kumabe, Yuto Ando, Yaqiang Liao, Yoshio Honda, Ya-Hong Xie, *Fellow, IEEE*, and Hiroshi Amano, *Member, IEEE*

***Abstract*—We demonstrated the formation of excellent Ohmic contact to *p*-type GaN (including the plasma etching-damaged *p*-type GaN which otherwise exhibited undetectable current within ±5 V) by the post-growth diffusion of magnesium. The specific contact resistivity on the order of 10^{-4} Ω.cm^2 (extracted at V = 0 V) was achieved on the plasma-damaged *p*-GaN with linear current-voltage characteristics by the transfer length method (TLM) measurement. The improvement in current by a factor of over 10^9 was also obtained on the plasma-damaged *p-n* junction diode after the same Mg-treatment. These experimental results indicate a great potential of post-growth diffusion of Mg to overcome the bottleneck of forming a good Ohmic contact to *p*-GaN.**

***Index Terms*—Diffusion processes, doping, gallium nitride, magnesium, Ohmic contacts.**

I. Introduction

GaN is a wide-bandgap semiconductor that experienced rapid development in optoelectronics and power electronics since the first demonstration of *p*-type conduction [1]. Until today, magnesium (Mg) is still the only dopant available to produce *p*-type GaN [2]. However, because of a high ionization energy (∼200 meV), the hole concentration is rather limited in even heavily doped *p*-GaN [3], [4]. Furthermore, the common and unavoidable plasma etching process easily introduce N-vacancy as compensating donor which reduces the hole concentration of the surface *p*-GaN and makes it act like lightly-doped *p*-GaN, leading to the increased difficulty of obtaining Ohmic contact to *p*-GaN [5]–[7]. As a result, a good Ohmic contact to *p*-GaN has become the bottleneck to improve the performance of related electronic devices such as merged PiN Schottky diode, *p-n* junction diodes, bipolar transistors and *p*-channel unipolar transistors (MISFET and HEMT) [8]–[14].

Doping by the post-growth diffusion is a common practice in semiconductors like Si. It produces a decaying dopant profile where the top of semiconductor was heavily doped with the dopants under constant source diffusion. Such degenerate semiconductor layer satisfies the regime to achieve the field-emission-induced carrier tunneling through the Schottky barrier and is critical to form a good metal-semiconductor Ohmic contact [15]–[17].

Post-growth diffusion by thermal annealing of Mg at high temperature and long time was reported to render *p*-type GaN [18]. In principle, the diffusion at low temperature and short time should be sufficient to build up a thin p^+ contact layer above existing bulk *p*-GaN to promote Ohmic contact, which could also subdue the compensating donors induced by plasma etch. Since the restoration of Ohmic contact to plasma-treated *p*-GaN is desired in the device processing stage, the post-growth diffusion of Mg with low annealing temperature and short time, if feasible, could also exhibit compatibility to a broad range of processing techniques.

In this letter, we demonstrated excellent Ohmic contact to *p*-GaN by post-growth diffusion of Mg at relatively low temperature and short time such as 550 °C and 10 min, even on the plasma-etched *p*-GaN. Furthermore, after the same Mg-treatment was used to recover the compromised Ohmic contact to *p*-layer of a GaN *p-n* junction diode (PND), the superior forward conduction further highlighted the good feasibility and effectiveness of the approach.

II. Experiments

The epi-layers consisting of ∼400 nm-thick *p*-type GaN with [Mg] = 7×10^{18} cm^{-3} and 2.5 μm-thick n^--type GaN with [Si] = 7×10^{16} cm^{-3} were grown by MOVPE on the ∼400 μm-thick 2 inch-diameter n^+-GaN substrate having free electron concentration of ∼10^{18} cm^{-3}. The top p^+ contact layer was not grown. The wafer was diced into dozens of small samples.

Fig. 1 (a)–(g) schematically illustrates the key steps in the fabrication flow for the *p*-GaN transfer length method (TLM) test structure and *p-n* junction diode. All the samples were annealed at T = 700 °C and t = 10 min in N_2 as a common step for *p*-GaN activation. Photolithography was utilized in (b), (d), and (f). Four paths were divided among the samples: I (blank): (a)-(b)-(f)-(g); II (Mg treatment only): (a)-(b)-(d)-(e)-(f)-(g); III (plasma treatment only): (a)-(b)-(c)-(f)-(g); IV (dual plasma and Mg treatment): (a)-(b)-(c)-(d)-(e)-(f)-(g). As shown in Fig. 1 (b), the Cl_2-based ICP-RIE was used for mesa etch (etching depth: ∼800 nm, hard mask: ∼3 μm photoresist) for the TLM test structure and the circular

Manuscript received November 11, 2021; accepted November 24, 2021. Date of publication November 25, 2021; date of current version December 29, 2021. This work was supported by the Japan's Ministry of Education, Culture, Sports, Science and Technology Program for Creation of Innovative Core Technology for Power Electronics under Grant JPJ009777. The review of this letter was arranged by Editor G. Han. *(Corresponding author: Jia Wang.)*

Jia Wang is with the Institute of Materials and Systems for Sustainability, Nagoya University, Nagoya, Aichi 464-8601, Japan, and also with the Department of Materials Science and Engineering, University of California at Los Angeles, Los Angeles, CA 90024 USA (e-mail: wang.jia@k.mbox.nagoya-u.ac.jp).

Shun Lu, Wentao Cai, Takeru Kumabe, and Yaqiang Liao are with the Department of Electronic Engineering, Graduate School of Engineering, Nagoya University, Nagoya, Aichi 464-8603, Japan.

Yuto Ando, Yoshio Honda, and Hiroshi Amano are with the Institute of Materials and Systems for Sustainability, Nagoya University, Nagoya, Aichi 464-8601, Japan.

Ya-Hong Xie is with the Department of Materials Science and Engineering, University of California at Los Angeles, Los Angeles, CA 90024 USA.

Color versions of one or more figures in this letter are available at https://doi.org/10.1109/LED.2021.3131057.

Digital Object Identifier 10.1109/LED.2021.3131057

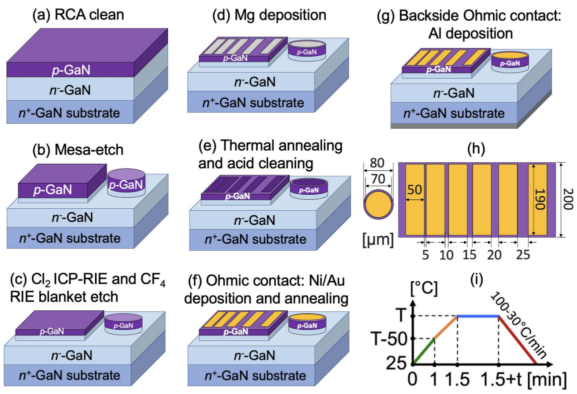

Fig. 1. (a)–(g) Schematic illustrations of the key steps of the fabrication flow for the *p*-GaN TLM test structure and *p-n* junction diode with plasma- and Mg-treatment. (h) Schematic plan-view of the TLM test structure and the mesa structure and anode of *p-n* junction diode. (i) Thermal cycle for all the annealing process mentioned in this letter with the defined variants of temperature (T) and time (t).

vertical *p-n* junction diode on the same sample (Fig. 1 (h)). For path III and IV designed to evaluate the effect of post-growth diffusion of Mg on the plasma-treated *p*-GaN, part of the samples were subject to the plasma treatment including Cl_2 ICP-RIE (ICP power: 150 W, bias power: 30 W, etching time: 30 s) followed by CF_4 RIE (bias power: 100 W, etching time: 2 min) which represent the most commonly used plasma etch methods in GaN processing technology (Fig. 1 (c)). Then, metallic pure Mg (50 nm) was patterned onto the *p*-GaN by sputtering except the blank samples as shown in Fig. 1 (d), followed by the annealing process in N_2 with the variants of temperature (T) and time (t). All the Mg-treated samples were cleaned by acid (HCl: H_2O_2: H_2O = 1:1:4) at 80 °C for 10 min to remove the residue metallic Mg and acid-soluble Mg compounds (Fig. 1 (e)). Finally, Ni (20 nm)/Au (150 nm) was E-beam evaporated onto all the samples at the exact same region with Mg and the alignment precision was within 1 μm, followed by thermal annealing with T = 525 °C and t = 5 min in O_2 (Fig. 1 (f) and (h)). Al (∼180 nm) was sputtered onto the backside of all the samples as the cathode for the PNDs (Fig. 1 (g)). In addition, a few samples underwent steps (a)-(d)-(e) (except that for (d), Mg was deposited on the entire sample surface) were measured by Secondary Ion Mass Spectroscopy (SIMS) to investigate the diffusion profile of Mg into GaN. In particular, these samples were polished and thinned to ∼1 μm before being sputtered from the backside during the SIMS to circumvent the possible interference of the topmost compound layer with high Mg content on the accurate determination of [Mg] in the underneath *p*-GaN layer.

III. Results and Discussion

Fig. 2 (a) is the *I-V* characteristic of the samples undergoing path I and path II with varying T. Both the path I sample (blank) and the path-II samples (T = 400 °C and 500 °C) did not exhibit Ohmic behavior. In stark contrast, the samples with 550 °C, 600 °C, and 700 °C exhibited excellent Ohmic behavior with fully linear *I-V* characteristics and the 800 °C sample also exhibited slightly degraded linearity. The transition between non-Ohmic to Ohmic occurred within 500 °C–550 °C, which was further revealed in Fig. 2. (b) featuring finer T steps. When T increased from 500 °C to 550 °C, the linearity of the *I-V* curves gradually improved. Furthermore, despite that 500 °C and 10 min led to non-Ohmic behavior, the sample with 500 °C and 60 min developed

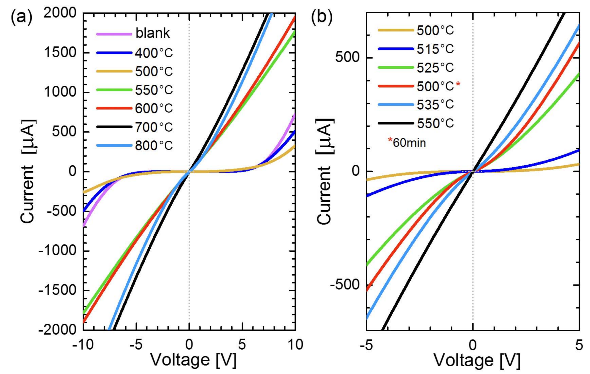

Fig. 2. (a) The *I-V* characteristics (contact spacing: 15 μm) of the blank sample and path II-samples with varying T (from 400 °C to 800 °C) and t = 10 min in the Mg-treatment process. (b) The *I-V* characteristics (contact spacing of 15 μm) of the path II-samples with T from 500 °C to 550 °C, t = 10 min, and T = 500 °C, t = 60 min.

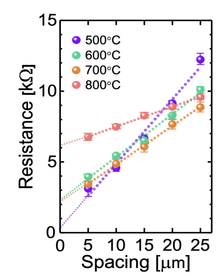

Fig. 3. The TLM results of the path-II samples with Mg-treatment (T = 550 °C, 600 °C, 700 °C, 800 °C) and t = 10 min, the resistance (R = dV/dI) was extracted at V = 0 V at steps of 25 mV.

TABLE I

The Sheet Resistance and the Specific Contact Resistivity of the Mg-Treated (Path-II) Samples

T and t	R_{sh} [kΩ/□]		ρ_c [Ω.cm²]	
550 °C, 10 min	V=0V	87.2	V=0V	2.59×10^{-4}
	V=±5V	70.5	V=±5V	5.21×10^{-5}
600 °C, 10 min	V=0V	57.6	V=0V	8.40×10^{-3}
	V=±5V	64.4	V=±5V	2.86×10^{-4}
700 °C, 10 min	V=0V	46.4	V=0V	1.29×10^{-2}
	V=±5V	51.5	V=±5V	1.33×10^{-3}
800 °C, 10 min	V=0V	24.6	V=0V	1.51×10^{-1}
	V=±5V	32.1	V=±5V	1.45×10^{-3}

improved Ohmic behavior with quasi-linear *I-V* curve. The fact that increasing the time could complement the otherwise insufficient temperature needed to form the Ohmic contact implied that diffusion of Mg in GaN was responsible for the observed Ohmic behavior.

Fig. 3 compares the TLM results (extracted at V = 0 V, step = 25 mV) of the path-II samples with T = 550 °C, 600 °C, 700 °C, and 800 °C and Table I summarizes the sheet resistance and the specific contact resistivity which were extracted both at V = 0 V and ±5 V (step = 25 mV). It is worth mentioning that the resistance (=dV/dI) tends to decrease gradually with increasing V. As a result, the specific contact resistivity exhibits lower value in general when extracted at higher voltages, and that extracted at V = 0 V represents an upper-bound value. It is concluded that with increasing temperature the sheet resistance decreased but the specific contact resistivity increased, which held true both for V = 0 V and ±5 V. The observed increase in the specific contact resistivity at higher temperature may be accounted for by the compound layer (chemically inert, insoluble in acids or alkalis) formed by interdiffusion of Mg and GaN on top of the

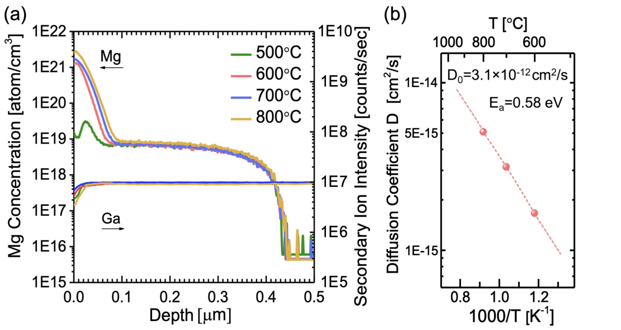

Fig. 4. (a) The SIMS profiles of Mg and Ga at varying annealing temperatures (T = 500 °C, 600 °C, 700 °C, 800 °C) and t = 10 min. (b) The temperature dependence of the extracted diffusion coefficient.

p-GaN which was thickened and coarsened with increasing T from 400 °C to 800 °C.

Fig. 4 (a) compares the diffusion profiles of Mg measured by the backside SIMS at varying annealing temperatures. The intensity of Ga decreased from 20–30 nm near the surface, corresponding to the compound layer featuring a mixture of GaN and Mg. The diffusion length L and total amount of diffused Mg increased with increasing T. The diffusion of Mg altered the previous distribution of [Mg] in the bulk p-GaN as more Mg diffused into p-GaN at higher T, thus giving rise to the hole concentration and decreasing the sheet resistance. On the other hand, the concomitant thickening of the parasitic compound layer on top of p-GaN gave rise to the specific contact resistivity in the same manner as did in the non-Ohmic range (400 °C to 500 °C) where the diffusion of Mg was insufficient to form the p^+-GaN layer. Compared to 500 °C, significant amount of Mg diffused into GaN for T = 600 °C, 700 °C, and 800 °C, forming p^+ contact layer in a top-down manner, resembling that by the bottom-up epitaxial growth of p^+-GaN. Based on the fitting of diffusion profiles with complementary error function for T = 600 °C, 700 °C, and 800 °C, Fig. 4 (b) estimated the pre-exponential factor D_0 and the activation energy for diffusion E_a by Eqn. (1):

$$D = D_0 \exp\left(-\frac{E_a}{kT}\right) \quad (1)$$

The low value of E_a (0.58 eV) in this range of T implied that the process was dominated by interstitial-dominated diffusion wherein most of diffused Mg atoms did not act as effective acceptors, and only a small amount of substitutional Mg_{Ga} contributed to the p^+-GaN layer [19]–[21].

Fig. 5 (a) compares the *I-V* results of the TLM test samples undergoing path III and path IV. It can be seen that the plasma-treated sample exhibited undetectable current within ±5 V (R > 1 TΩ), proving that the Ohmic contact to p-GaN was seriously compromised by the etching-induced damages. Then, after Mg-treatment at 550 °C (10 min), the ideal Ohmic contact with fully linear *I-V* curve was restored, similar to that of the path II-sample in Fig. 3. As shown by the TLM result (extracted at V = 0 V, step = ±25 mV) in Fig. 4 (b), the sheet resistance was 127.5 kΩ/sq and the specific contact resistivity was 3.55×10^{-4} Ω.cm^2. Since the Cl_2 ICP-RIE process also thinned the p-GaN by ~120 nm (etching rate: 4 nm/s, time: 30 s), the ratio of the increased p-GaN sheet resistance (127.5/87.2 × 100% = 146%) well matched that of the reduced p-thickness (400/280 × 100% = 143%), which proved good repeatability of the experiments.

Fig. 6 (a) compares the *I-V* characteristics of the PNDs undergoing path I (blank), II (Mg-treated only, T = 550 °C), III (plasma-treated only), and path IV (dual plasma-and-Mg-treated, T = 550 °C), respectively. Both path II- and path IV-PNDs exhibited similar and drastically improved current compared to path I- and path III-PNDs. As shown in Fig. 6 (b), a low turn-on voltage of 3 V, an ultra-low ideality factor (IF) of 1.3 for GaN PND at 2.9 V, and a high current density J of 1 kA/cm^2 at 3.5 V (mesa area is taken as device area, diameter: 80 μm) were obtained on the dual plasma-Mg-treated PND, owing to the excellent Ohmic contact formed onto p-GaN [22]–[24]. Compared to path II-PND, path IV-PND showed slightly increased current because of the reduced series resistance of thinned p-layer in a vertical PND by the Cl_2 ICP-RIE process. This also proved in the vertical current path that the post-growth diffusion of Mg was effective to perfectly restore the ideal Ohmic contact to the plasma-etched p-GaN.

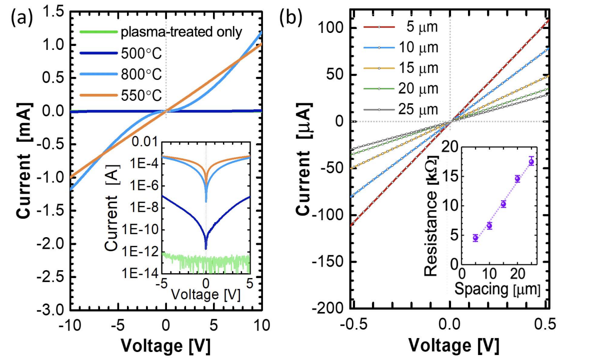

Fig. 5. (a) The *I-V* characteristics (contact spacing of 15 μm) of path-III sample (plasma-treated only) and path-IV samples (with plasma and Mg-treatment (varying T and t = 10 min)). (b) TLM result of the plasma-treated sample after Mg-treatment (T = 550 °C and t = 10 min).

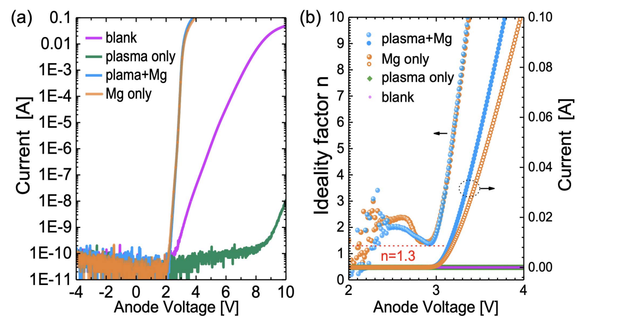

Fig. 6. (a) The semilogarithmic *I-V* characteristics of the PNDs (blank, plasma-treated only, Mg-treated only, and dual plasma-Mg-treated, respectively). (b) The ideality factor and the forward *I-V* characteristic curves of corresponding PNDs plotted in linear scale.

IV. Conclusion

In summary, we demonstrated excellent Ohmic contact to p-GaN by post-growth diffusion of Mg at relatively low temperature and short time, even after it was subject to the plasma etching-induced damages which otherwise exhibited undetectable current within ±5 V (R> 1 TΩ). The specific contact resistivity as low as 0.5–2.6 × 10^{-4} Ω.cm^2 was extracted at the low voltage (≤5 V) by TLM measurement. The superior forward *I-V* characteristics of the p-$n$junction diode further highlighted the benefit of the excellent Ohmic contact to p-GaN. The good feasibility and effectiveness of such approach may indicate a great potential in overcoming the bottleneck of Ohmic contact to p-type GaN.

References

[1] H. Amano, M. Kito, K. Hiramatsu, and I. Akasaki, "P-type conduction in Mg-doped GaN treated with low-energy electron beam irradiation (LEEBI)," *Jpn. J. Appl. Phys.*, vol. 28, no. 12, pp. L2112–L2114, Dec. 1989, doi: 10.1143/JJAP.28.L2112.

[2] M. A. Reshchikov, P. Ghimire, and D. O. Demchenko, "Magnesium acceptor in gallium nitride. I. Photoluminescence from Mg-doped GaN," *Phys. Rev. B, Condens. Matter*, vol. 97, no. 20, May 2018, Art. no. 205204, doi: 10.1103/PhysRevB.97.205204.

[3] W. Götz, N. M. Johnson, J. Walker, D. P. Bour, and R. A. Street, "Activation of acceptors in Mg-doped GaN grown by metalorganic chemical vapor deposition," *Appl. Phys. Lett.*, vol. 68, no. 5, pp. 667–669, Jan. 1996, doi: 10.1063/1.116503.

[4] S. Brochen, J. Brault, S. Chenot, A. Dussaigne, M. Leroux, and B. Damilano, "Dependence of the Mg-related acceptor ionization energy with the acceptor concentration in P-type GaN layers grown by molecular beam epitaxy," *Appl. Phys. Lett.*, vol. 103, no. 3, pp. 1–5, Jun. 2013, doi: 10.1063/1.4813598.

[5] Z.-Q. Fang, D. C. Look, X.-L. Wang, J. Han, F. A. Khan, and I. Adesida, "Plasma-etching-enhanced deep centers in N-GaN grown by metalorganic chemical-vapor deposition," *Appl. Phys. Lett.*, vol. 82, no. 10, pp. 1562–1564, Mar. 2003, doi: 10.1063/1.1560562.

[6] X. A. Cao, S. J. Pearton, A. P. Zhang, G. T. Dang, F. Ren, R. J. Shul, L. Zhang, R. Hickman, and J. M. Van Hove, "Electrical effects of plasma damage in P-GaN," *Appl. Phys. Lett.*, vol. 75, no. 17, pp. 2569–2571, Oct. 1999, doi: 10.1063/1.125080.

[7] T. Kumabe, Y. Ando, H. Watanabe, M. Deki, A. Tanaka, S. Nitta, Y. Honda, and H. Amano, "Etching-induced damage in heavily Mg-doped P-type GaN and its suppression by low-bias-power inductively coupled plasma-reactive ion etching," *Jpn. J. Appl. Phys.*, vol. 60, May 2021, Art. no. SBBD03, doi: 10.35848/1347-4065/abd538.

[8] J. Wang, Y.-H. Xie, and H. Amano, "High-gain gated lateral power bipolar junction transistor," *IEEE Electron Device Lett.*, vol. 42, no. 9, pp. 1370–1373, Sep. 2021, doi: 10.1109/led.2021.3099982.

[9] T. Hayashida, T. Nanjo, A. Furukawa, and M. Yamamuka, "Vertical GaN merged PiN Schottky diode with a breakdown voltage of 2 kV," *Appl. Phys. Exp.*, vol. 10, no. 6, p. 061003, May 2017, doi: 10.7567/APEX.10.061003.

[10] S. Kawasaki, Y. Ando, M. Deki, H. Watanabe, A. Tanaka, S. Nitta, Y. Honda, M. Arai, and H. Amano, "Experimental demonstration of GaN IMPATT diode at X-band," *Appl. Phys. Exp.*, vol. 14, no. 4, p. 46501, 2021, doi: 10.35848/1882-0786/abe3dc.

[11] S.-C. Shen, R. D. Dupuis, Z. Lochner, Y.-C. Lee, T.-T. Kao, Y. Zhang, H.-J. Kim, and J.-H. Ryou, "Working toward high-power GaN/InGaN heterojunction bipolar transistors," *Semicond. Sci. Technol.*, vol. 28, no. 7, Jul. 2013, Art. no. 074025, doi: 10.1088/0268-1242/28/7/074025.

[12] B. F. Chu-Kung, C. H. Wu, G. Walter, M. Feng, N. Holonyak, T. Chung, J.-H. Ryou, and R. D. Dupuis, "Modulation of high current gain (β> 49) light-emitting InGaN/GaN heterojunction bipolar transistors," *Appl. Phys. Lett.*, vol. 91, no. 23, Dec. 2007, Art. no. 232114, doi: 10.1063/1.2821380.

[13] M. Hua, J. Chen, C. Wang, L. Liu, L. Li, J. Zhao, Z. Jiang, J. Wei, L. Zhang, Z. Zheng, and K. J. Chen, "E-mode P-GaN gate HEMT with p-FET bridge for higher V_{TH} and enhanced V_{TH} stability," in *IEDM Tech. Dig.*, Dec. 2020, pp. 21–23, doi: 10.1109/IEDM13553.2020.9371969.

[14] N. Chowdhury, Q. Xie, M. Yuan, N. S. Rajput, P. Xiang, K. Cheng, H. W. Then, and T. Palacios, "First demonstration of a self-aligned GaN p-FET," in *IEDM Tech. Dig.*, Dec. 2019, pp. 4–6, doi: 10.1016/0038-1101(66)90097-9.

[15] F. A. Padovani and R. Stratton, "Field and thermionic-field emission in Schottky barriers," *Solid-State Electron.*, vol. 9, no. 7, pp. 695–707, 1966, doi: 10.1016/0038-1101(66)90097-9.

[16] D. K. Schroder, *Semiconductor Material and Device Characterization*. Hoboken, NJ, USA: Wiley, 2006.

[17] G. Greco, F. Iucolano, and F. Roccaforte, "Ohmic contacts to gallium nitride materials," *Appl. Surf. Sci.*, vol. 383, pp. 324–345, Oct. 2016, doi: 10.1016/j.apsusc.2016.04.016.

[18] Y. J. Yang, J. L. Yen, F. S. Yang, and C. Y. Lin, "P-type GaN formation by Mg diffusion," *Jpn. J. Appl. Phys., Lett.*, vol. 39, no. 5, pp. 7–10, 2000, doi: 10.1143/jjap.39.l390.

[19] P. Shewmon, *Diffusion in Solids*. Cham, Switzerland: Springer, 2016.

[20] C. J. Pan and G. C. Chi, "The doping of GaN with Mg diffusion," *Solid-State Electron.*, vol. 43, no. 3, pp. 621–623, 1999, doi: 10.1016/S0038-1101(98)00289-5.

[21] K. Harafuji and K. Kawamura, "Magnesium diffusion at dislocation in wurtzite-type GaN crystal," *Jpn. J. Appl. Phys.*, vol. 44, no. 9, pp. 6495–6504, Sep. 2005, doi: 10.1143/JJAP.44.6495.

[22] R. Abdul Khadar, C. Liu, L. Zhang, P. Xiang, K. Cheng, and E. Matioli, "820-V GaN-on-Si quasi-vertical pin diodes with BFOM of 2.0 GW/cm^2," *IEEE Electron Device Lett.*, vol. 39, no. 3, pp. 401–404, Mar. 2018, doi: 10.1109/LED.2018.2793669.

[23] K. Nomoto, B. Song, Z. Hu, M. Zhu, M. Qi, N. Kaneda, T. Mishima, T. Nakamura, D. Jena, and H. G. Xing, "1.7-kV and 0.55-mΩ·cm^2 GaN pn diodes on bulk GaN substrates with avalanche capability," *IEEE Electron Device Lett.*, vol. 37, no. 2, pp. 161–164, Dec. 2015, doi: 10.1109/LED.2015.2506638.

[24] J. M. Shah, Y. Li, T. Gessmann, and E. Fred Schubert, "Experimental analysis and a new theoretical model for anomalously high ideality factors (n$\gg$2.0) in GaN-based pn junction diodes," *MRS Proc.*, vol. 798, pp. 2627–2630, Dec. 2003, doi: 10.1557/proc-798-y7.11.